# VALIDATION OF A LOW-FIDELITY TOOL FOR SIZING LOADS PREDICTION ACROSS MULTIPLE AIRCRAFT ARCHITECTURES

**Matteo Manfredi**
Leonardo Helicopter Division
Cascina Costa (VA), Italy

**Thomas Soprani**
Leonardo Helicopter Division
Cascina Costa (VA), Italy

**Carlo Mazzoli**
Leonardo Helicopter Division
Cascina Costa (VA), Italy

**Riccardo Piani**
Leonardo Helicopter Division
Cascina Costa (VA), Italy

## ABSTRACT

An efficient conceptual design phase must be characterized by fast and reliable procedures that can produce high-level sensitivity analysis and assess the impact of design variations. The increasing complexity of aircraft architecture requires multipurpose solutions that go beyond simple approaches such as regression models, demanding more flexible techniques for route design exploration. This paper presents the specifications of a Python-based airframe loads analysis tool, TONALE, which aims to predict the sizing conditions and associated loads that act on an aircraft. Starting from inputs readily available from the very first iterations, this tool can perform low-fidelity aerodynamic analysis and structural evaluations on a reduced-order model of both traditional and unconventional configurations.

The objective is to discuss the results in terms of sizing envelopes by highlighting both the capabilities and the criticalities that emerged during the validation process, for different components and architectures.

## NOTATION

*

Symbols

$\vec{x}_{cg}$ Position of CG

$m_i$ Element of mass

$\vec{p}_i$ Position of i-th mass element

$d_{ix}$ X distance of the i-th element from the CG

$d_{iy}$ Y distance of the i-th element from the CG

$d_{iz}$ Z distance of the i-th element from the CG

$\mathbf{J}$ Inertial tensor

$\mathbf{J_i}$ Inertial tensor of the i-th mass element

$\vec{\ddot{x}}_{cg}$ CG linear acceleration

$\vec{\omega}_{cg}$ CG angular rate

$\vec{\dot{\omega}}_{cg}$ CG angular acceleration

$R$ Rotor radius, m

$\vec{F}_{ext}$ External resultant forces

$\vec{M}_{ext}$ External resultant moment

$M$ Aircaft mass

$\vec{F}_{aero}$ Resultant aerodynamic forces

$\vec{F}_{LG}$ Resultant landing gear forces

$\vec{F}_{prop}$ Resultant propulsive forces

$\vec{F}_i$ Forces acting on i-th mass element

$\vec{M}_i$ Moments acting on i-th mass element

$\vec{a}_i$ Local acceleration evaluated for the i-th mass element

$a_{ix}$ X acceleration of the i-th mass element

$a_{iy}$ Y acceleration of the i-th mass element

$a_{iz}$ Z acceleration of the i-th mass element

$P_{hp}$ Engine Installed Power, HP

$T_{des}$ Design Torque

$\sigma$ Rotor solidity

$\eta_p$ Propulsive efficiency

$n_x$ Longitudinal Load factor, g

$n_y$ Lateral Load factor, g

$n_z$ Vertical Load factor, g

$\dot{p}$ Roll angular rate, 1/s

$\dot{q}$ Pitch angular rate, 1/s

$\dot{r}$ Yaw angular rate, 1/s

$\ddot{p}$ Roll angular acceleration, $1/s^2$

$\ddot{q}$ Pitch angular acceleration, $1/s^2$

$\ddot{r}$ Yaw angular acceleration, $1/s^2$

$\vec{N_{LG}}$ Nose landing gear reaction

$\vec{M_{LGL}}$ Left landing gear reaction

$\vec{M_{LGR}}$ Right landing gear reaction

$\vec{T_{LG}}$ Tail landing gear reaction

*

Acronyms

**ERF** European Rotorcraft Forum

**LHD** Leonardo Helicopter Division

**ROM** Reduced Order Model

**DOF** Degrees of Freedom

**MTOW** Maximum Take-off weight

**CG** Center of Gravity

**STA** STAtion

**Bl** Butt Line

**AB-Method** Acceleration based method

**VTOL** Vertical Take-off and Landing

**AP-mode** Airplane Mode

**LG** Landing Gear

# INTRODUCTION

Evaluating sizing loads for a new aircraft has consistently been a critical phase in the aircraft design process (Ref. 1).
Overly conservative estimations of load levels can lead to structural overdesign, resulting in penalties concerning both payload and performance.
In contrast, underestimating design loads may lead to solutions that are unacceptable from a safety perspective and in terms of regulatory compliance.
Consequently, various methodologies have been developed over the years to estimate sizing loads as accurately as possible, even in the preliminary design stages, by leveraging recurring architectural concepts.
However, sizing load estimation remains a pivotal phase in aircraft design, demanding significant computational effort. This is because the number of load cases required for analysis to achieve accurate results often spans tens of thousands at each design iteration (Ref. 2). Accurately identifying the most critical conditions for a given structure, while significantly impacting the development costs of a new aircraft, guides both the selection of appropriate materials and the evaluation of architectural choices. This enables the selection of optimal solutions in terms of development and operational costs throughout the entire project lifecycle (Ref. 3).
In recent years, however, the proliferation of innovative architectures has raised concerns regarding the applicability of conventional methodologies to new concepts. This has highlighted questions about the confidence and robustness that established sizing load estimation processes can offer when faced with innovative aircraft configurations.
In response to this scenario, the TONALE (Tool for cONceptual Airframe Loads Evaluation) simulation tool has been developed within Leonardo Helicopter Division.TONALE estimates airframe sizing loads for new aircraft concepts, seeking to overcome the limitations of standard approaches in terms of both computational and economic costs, as well as result accuracy, while enabling deeper design space exploration through sensitivity analysis of key aircraft design parameters.
The purpose of this work is to briefly introduce the capabilities of TONALE, while presenting the verification & validation activities carried out during the late development stage of the software.

# TONALE

TONALE is a simulation code developed in Python, based on an enforced acceleration methodology, which belongs to the class of low-fidelity approaches.
Starting with creating a Reduced Order Model (ROM) of the aircraft, the tool predicts aerodynamic and inertial loads on airframe components and identifies sizing conditions for both conventional and unconventional aircraft, delivering reliable results within timeframes suitable for preliminary and conceptual design iterations. This enables preliminary load analysis within a time frame of minutes, compared to the weeks typically required by traditional methods.

### Process overview

Figure 1 illustrates the process overview, which starts with preliminary mass distributions and aircraft geometrical description. These inputs are used to assemble the ROM of the aircraft.
The identification of tailored design flight envelopes is performed by considering the specific aircraft type, required performance characteristics, applicable regulations, and LHD internal know-how. A simplified physics-based control allocation is assumed, allowing the trim problem to not be reliant

on complex fly-by-wire control logics that may not be available in the early design stages. Following this approach, each aircraft's macro-item (wing, tail, rotors, etc.) can generate control moments according to its physical behavior, modeled with a binary logic that enables and disables its influence on a specific degree of freedom (DOF).
A mathematical solution of the 6 DOF accelerated trim is evaluated by computing aerodynamic and propulsive forces to match the CG-enforced target accelerations.

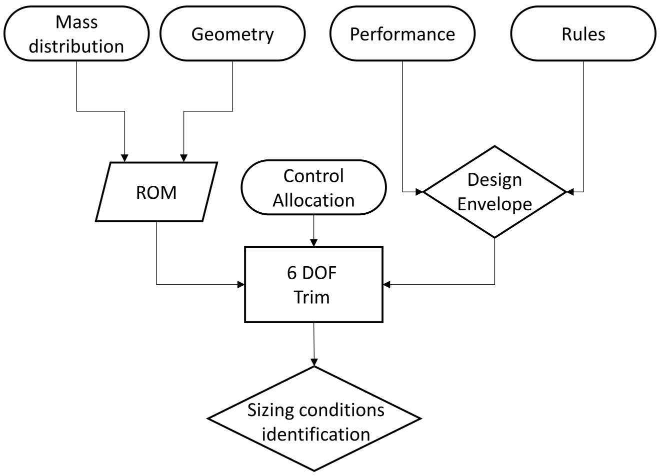


**Figure 1. Process flow-chart**

By combining rates and accelerations, it is possible to cover all operative conditions, from structural flight maneuvers (including gust analysis) to landing and ground handling.
Limit loads for each aircraft component are subsequently defined, and sizing conditions for each airframe macro-item are identified.

### ROM model characteristics

To generate the loadset the ROM includes the following schematization:

1. Low-fidelity (Ref. 4) aerodynamic model is applied. Lifting surfaces are modeled as lifting lines, with their aerodynamic coefficients computed by basic approximations (Ref. 5) (Ref. 6).

2. Rigid stick-beam airframe, representative of structural elements, is taken into account.

3. Non-structural elements (subsystems, fuel, payload, etc.) are rigidly connected to the stick beam model and taken into account by considering only their inertial characteristics.

4. Propulsive elements are taken into account and act by their forces and moments.

### Trim solution

The position of the CG and the inertial tensor of the aircraft are evaluated according to the given mass distribution, with Equation 1 and Equation 2.

$$\vec{x}_{cg} = \frac{\sum_{i=1}^{n} m_i \vec{p}_i}{\sum_{i=1}^{n} m_i} \quad (1)$$

$$J = \begin{pmatrix} \sum_{i=1}^{n} m_i d_{ix}^2 & -\sum_{i=1}^{n} m_i d_{ix} d_{iy} & -\sum_{i=1}^{n} m_i d_{ix} d_{iz} \\ -\sum_{i=1}^{n} m_i d_{ix} d_{iy} & \sum_{i=1}^{n} m_i d_{iy}^2 & -\sum_{i=1}^{n} m_i d_{iy} d_{iz} \\ -\sum_{i=1}^{n} m_i d_{ix} d_{iz} & -\sum_{i=1}^{n} m_i d_{iy} d_{iz} & \sum_{i=1}^{n} m_i d_{iz}^2 \end{pmatrix} \quad (2)$$

The aircraft CG is subjected to the enforced acceleration field, and its motion must satisfy the Equations in 3.

$$\begin{cases} \vec{F_{ext}} = M\ddot{\vec{x}}_{cg} \\ \vec{M_{ext}} = \mathbf{J}\dot{\vec{\omega}}_{cg} + \mathbf{rJ}\vec{\omega}_{cg} \end{cases} \quad (3)$$

Where:

$$\mathbf{r} = \vec{\omega}_{cg} \cdot \begin{pmatrix} 0 & -1 & 1 \\ 1 & 0 & -1 \\ -1 & 1 & 0 \end{pmatrix} \quad (4)$$

External forces can be rewritten as per Equation 5.

$$\vec{F_{ext}} = \vec{F_{aero}} + \vec{F_{LG}} + \vec{F_{prop}} \quad (5)$$

Aerodynamic and propulsive forces in flight are computed such that CG target accelerations are enforced along the six DOFs, under the preliminary control logic specified among the inputs.

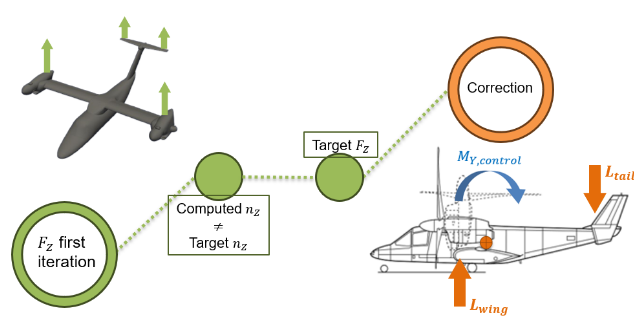


**Figure 2. TONALE matching of external forces with enforced acceleration field**

Target accelerations are stated as input parameters, but they are automatically updated to take into account possible unexpected deviations from these predefined values, such as gusts increasing the maximum vertical load factor.
After completing the trim analysis, each aerodynamic component generates a sextuple of forces and moments applied to

the mean aerodynamic chord. To have a more realistic representation of aerodynamic loads, they are distributed along the component by an optimization procedure, in which a cost function is defined for three rotational DOFs. By imposing the number of grid points among which loads are distributed, each cost function can be formulated as the difference between the moment generated by the single sextuple along one DOF and the sum of forces (or moments) generated by all grids modeling the evaluated aerodynamic component. Equation 6 shows the expression of the cost function associated with the roll DOF: $d$ and $L$ are known, the first being the distance of the $i_{th}$ grid point from the aircraft CG while the second being the rolling moment generated by the actual analyzed component (output of trim analysis); $F_{(z,i)}$ and $F_{(y,i)}$ are unknown forces (optimization outputs) applied to the $i_{th}$ grid.

$$F_{cost} = \mathbf{L} - \left( \sum_{1}^{ngrid} F_{z,i} d_{y,i} + F_{y,i} d_{z,i} \right) \tag{6}$$

It is possible to specify the desired distribution type among different options (uniform, elliptical, linear): this translates to different constraints applied during optimization. The fulfillment of dynamic equilibrium along translational DOFs after the optimization is granted by enforcing the sum of all the forces applied to the i-th grid to be equal to the original single vector of forces generated by the component. Landing gear reactions, used to evaluate landing and ground handling loads, are applied at ground contact points and, in general, are given by Equation 7.

$$\vec{F_{LG}} = \vec{N_{LG}} + \vec{M_{LGL}} + \vec{M_{LGR}} + \vec{T_{LG}} \tag{7}$$

Design propulsive forces are expressed as in Equation 8.

$$\vec{F_{prop}} = f\left(R, \sigma, P_{hp}, \eta_p, T_{des}\right) \tag{8}$$

Consequently, these are evaluated according to the enforced acceleration field required and aerodynamic forces evaluated in Figure 2.

### Sizing loads evaluation

Resultant shear forces and bending moments (internal actions) are evaluated on the reference stick beam for each airframe element, by integrating the contribution of:

- Aerodynamic forces;
- Propulsive forces;
- Inertial loads of the mass elements.

The contribution of inertial loads due to the i-th element of masses is evaluated in Equation 9, taking into account local accelerations, determined as per Equation 10.

$$\begin{cases} \vec{F_i} = -\vec{a_i} m_i \\ \vec{M_i} = -\mathbf{J}_i \vec{\dot{\omega}_{cg}} + \mathbf{r}\mathbf{J}_i \vec{\omega_{cg}} \end{cases} \tag{9}$$

$$\begin{cases} a_{ix} = \vec{\ddot{x}_{cg}} - \left(q^2 + r^2\right) d_{ix} + \left(pq - \dot{r}\right) d_{iy} + \left(pr - \dot{q}\right) d_{iz} \\ a_{iy} = \vec{\ddot{y}_{cg}} + \left(pq + \dot{r}\right) d_{ix} - \left(p^2 + r^2\right) d_{iy} + \left(qr - \dot{p}\right) d_{iz} \\ a_{iz} = \vec{\ddot{z}_{cg}} + \left(pr + \dot{q}\right) d_{ix} + \left(qr + \dot{p}\right) d_{iy} - \left(p^2 + q^2\right) d_{iz} \end{cases} \tag{10}$$

A proven process for sizing loads selection, based on LHD heritage and know-how, is embedded inside the tool. This allows for the automatic identification of the design condition for the different airframe components in the main section of interest for each. The corresponding load cases are then compiled into an output file, suitable for input into standard FEM solver.

### Computational performances

Computational effort required for a complete airframe loads assessment performed in the TONALE environment with respect to conventional airframe loads methods up to 1000 times more time efficient, as presented in Figure 3, enabling a full exploration of several design solutions in the typical timeframe of a conceptual or preliminary design study.

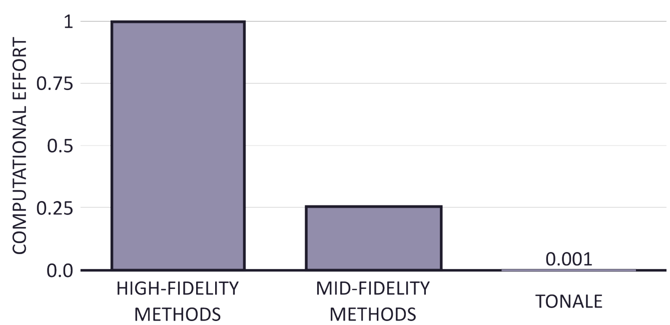


**Figure 3. Comparison of computational effort between TONALE and conventional approaches**

## VALIDATION RESULTS

In the following paragraphs, the main results produced during the TONALE verification and validation activity are presented. In particular, the focus is on results obtained for both conventional and transformative aircrafts. For the main airframe components, the overall error between all static loads predicted with Tonale and the same quantity obtained with a high-fidelity approach is presented. A positive percentage means a conservative solution obtained with TONALE. The figures present the maximum error at the specified adimensionalized STA (STAtion) or BL (Butt Line). Tables presented in Appendix summarize and split the errors for each different sizing load which directly impacts structural sizing and aircraft empty weight.

### AW609

For the AW609, the focus is on the deltas between the sizing conditions for the wing, fuselage, fin, and horizontal tail.

Figure 4 shows that predicted loads along the wing are generally conservative compared to the reference values. Errors exceeding 15% for the case of sizing load 2 (see Section 6, Table 4) result from significant discrepancies between the conceptual mass distributions and more representative ones. At the root, where the influence of a non-fully representative mass distribution is limited, the error decreases. However, it must be noted that the sizing load 2 has a second-order effect with respect to the sizing envelope, while the more relevant sizing loads show a maximum error of about 8%.

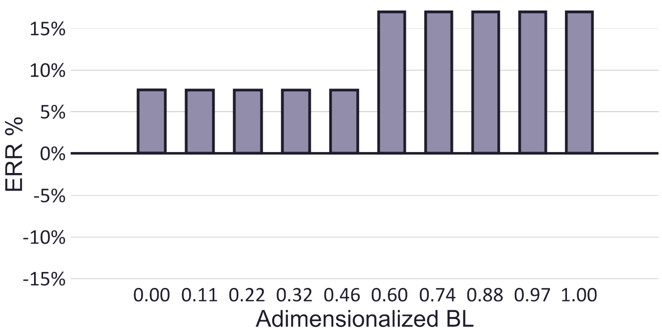


**Figure 4. AW609 Wing - Maximum overall error in different sizing loads**

In some section of the fuselage and fin, there are negative errors in estimating the sizing loads (Figure 5) (Figure 7). These are likely caused by the error affecting the aerodynamic loads generated by the horizontal stabilizer (Figure 6 and Section 6). To minimize computational cost, the model's masses are translated into a coarse mass distribution where mass is lumped at the center of each octree box representing that component. Since the maximum number of masses per box is fixed, box dimensions increase near the element's tip, causing tip masses to shift toward the root and resulting in load underestimation in these areas.

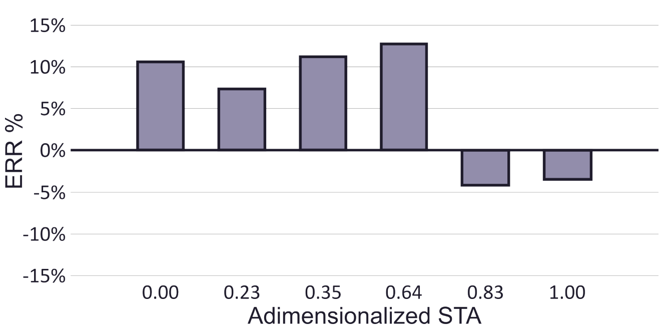


**Figure 5. AW609 Fuse - Maximum overall error in different sizing loads**

Although errors approach 20% in some sections, the main sizing load for each component determined by the combination of loads from the most severe load case, is consistently predicted with less than 10% error, as shown in Table 1. Positive errors indicate conservative load estimates.

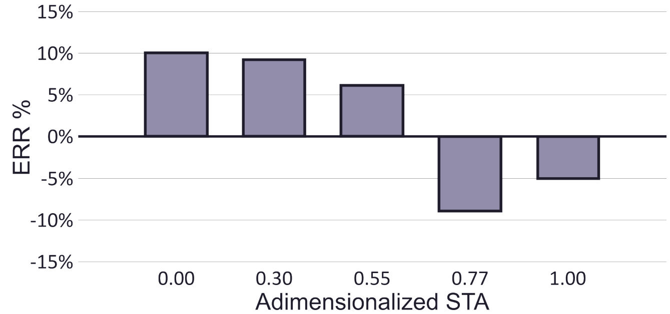


**Figure 6. AW609 HT - Maximum overall error in different sizing loads**

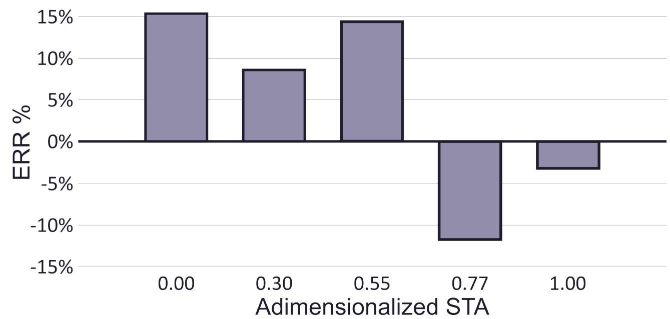


**Figure 7. AW609 Fin - Maximum overall error in different sizing loads**

**Table 1. Maximum error in the identified most severe load case subdivided by components**

| Wing | Fuselage | Fin | HT |
|---|---|---|---|
| 7.8% | -5.2% | 7.0% | 8.1% |

### NGCTR-TD

For the NGCTR-TD, the focus is on the deltas between the sizing conditions for the wing, fuselage, and fin.

As Figure 8 presents, TD's wing is highlighting a 10% increase in maximum loads at the root station. Since Tonale serves as a conceptual design tool, an overestimate of 10% is appropriate and acceptable.

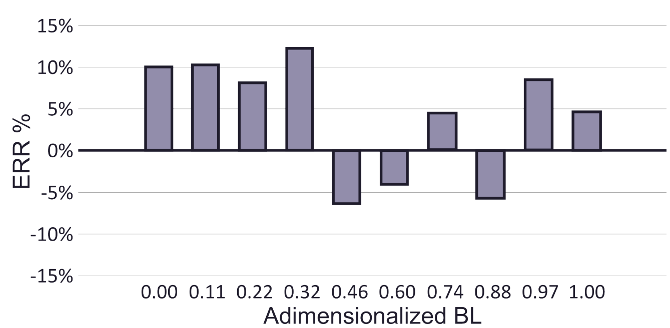


**Figure 8. NGCTR-TD Wing - Maximum overall error in different sizing loads**

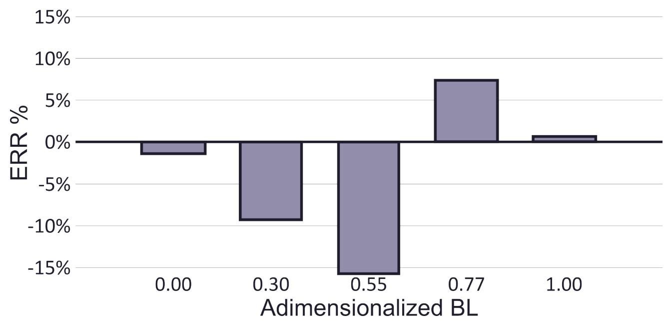


**Figure 9. NGCTR-TD Fin - Maximum overall error in different sizing loads**

The fuselage errors, depicted in Figure 10 highlight a marked error band, especially in the initial part. This is derived from the forces introduced by the landing gear, where Tonale results are much more conservative. This is an expected results since the dataset used for comparison is missing the sizing loads specific for that section.

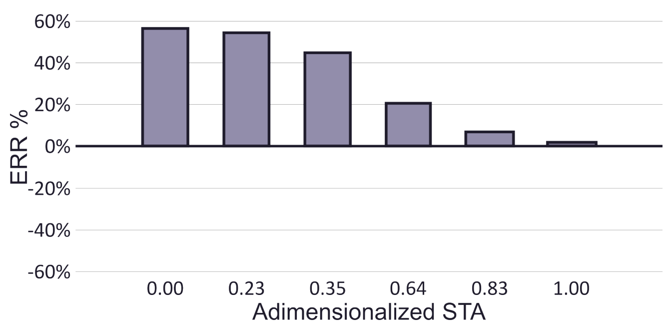


**Figure 10. NGCTR-TD Fuse - Maximum overall error in different sizing loads**

**Table 2. Maximum error in the identified most severe load case subdivided by components**

| Wing | Fuselage | Fin |
|---|---|---|
| 12.0% | 18.0% | 2.40% |

### AW139

For the AW139, the focus is on deltas between sizing conditions for the tail boom. For the three main sizing loads presented, TONALE predicts with a reasonable level of accuracy the design load, with the majority of the results highlighting a conservative output. Only for sizing loads 2, as presented in Table 8, prediction at adimensional STA = 0 and at adimensional STA = 0.83 is on the non-conservative side. This has been found to be related to local effects, justified by the introduction of external loads from other components.

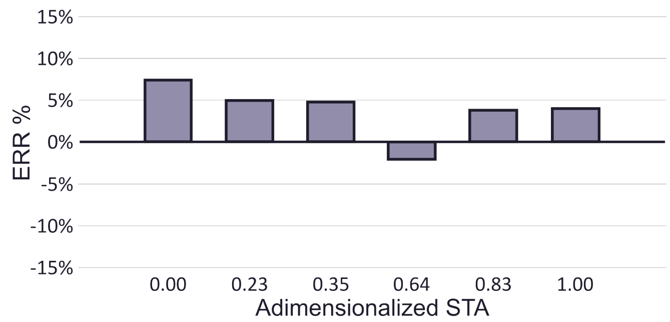


**Figure 11. AW139 Fuse - Maximum overall error in different sizing loads**

**Table 3. Maximum error in the identified most severe load case subdivided by components**

| Fuselage |
|---|
| 4.70% |

### GENERIC TILT ROTOR

The maximum error can be found at the wingtip. The error is linked to the mass distribution discrepancies as widely described in the AW609 results, while the differences at the root are to be considered within the acceptable limits of the method's discretization.

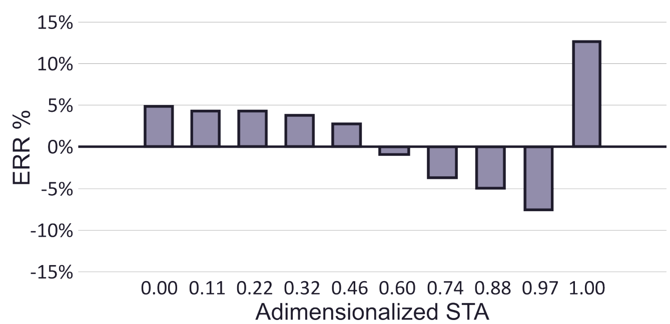


**Figure 12. Generic Tiltrotor Wing - Maximum overall error in different sizing loads**

## CONCLUSIONS

TONALE offers an innovative environment and method to evaluate airframe sizing loads, in particular:

1. TONALE is deemed capable of modeling successfully both conventional and transformative aircraft configurations.
2. Sizing conditions are correctly identified.
3. Sizing load predictions for all airframe components are comparable to those obtained with higher-fidelity methods. The highest errors recorded (especially in the case of NGTRD-TD fuselage) are explained by the lack of

the most severe load cases in the envelopes used as reference: in fact, TONALE is tuned such that the computed loads cover all the operative conditions of the aircraft; a re-combination of rates and accelerations is needed if some kind of manoeuvres or landings are not included in the analysis.

4. The presented results demonstrate that TONALE achieves the accuracy and computational efficiency required for conceptual and preliminary design applications.

5. The demonstrated performance makes TONALE suitable for multidisciplinary optimization environments, supporting rapid design iterations and enhanced structural design efficiency.

Author contact:
Matteo Manfredi matteo.manfredi01@leonardo.com
Thomas Soprani thomas.soprani@leonardo.com
Carlo Mazzoli carlo.mazzoli@leonardo.com
Riccardo Piani riccardo.piani@leonardo.com

## ACKNOWLEDGMENTS

The Authors would like to express their gratitude to Leonardo Helicopter Division and the Aircraft System Integration (ASI) Department their gratitude for allowing the project on TONALE to be developed and presented at ERF 2025.

## REFERENCES

1. Castagne, S., Curran, R., Rothwell, A. et al. *A generic tool for cost estimating in aircraft design* Res Eng Design 18, 149–162 (2008). https://doi.org/10.1142/p987

2. Castellani, M., Lemmens, Y., and Cooper, J., *Reduced Order Model Approach for Efficient Aircraft Loads Prediction*, SAE Int. J. Aerosp. 8(2):273-281, 2015, https://doi.org/10.4271/2015-01-2568

3. Gyazova, M.M., Siluyanova, M.V., Bondaren-ko, D.A. et al., *Cost Management over the Aircraft Life Cycle*. Russ. Engin. Res. 40, 1030–1033 (2020). https://doi.org/10.3103/S1068798X20120059

4. Leifsson, L. and Koziel, S. *Simulation-Driven Aerodynamic Design Using Variable-Fidelity Models*, Imperial College Press (2015). https://doi.org/10.1142/p987

5. Prandtl, L. and Tietjins, O.G., *Applied Hydro-and Aeromechanics*, United Engineering Trustees, Inc., 1934. https://archive.org/details/in.ernet.dli.2015.205401

6. Prandtl, L., Tragflügeltheorie. I. Mitteilung. *Nachrichten von der Gesellschaft der Wissenschaften zu Göttingen*, Mathematisch-Physikalische Klasse 1918 (1918): 451-477. http://eudml.org/doc/59036

## CLASSIFICATION & COPYRIGHT

## APPENDIX

**Table 4. Maximum error about sizing loads subdivided by adimensionalized BL - AW609 Wing**

| SZ loads | 0.00 | 0.11 | 0.46 | 0.74 | 1.00 |
|---|---|---|---|---|---|
| ID 1 | 5.4% | 5.7% | 2.9% | -2.9% | 0.6% |
| ID 2 | 8.2% | 8.2% | 8.3% | 18.7% | 18.7% |
| ID 3 | -5.3% | -3.8% | 2.8% | 5.9% | -4.6% |

**Table 5. Maximum error about sizing loads subdivided by adimensionalized STA - AW609 Fuselage**

| SZ loads | 0.00 | 0.23 | 0.35 | 0.64 | 1.00 |
|---|---|---|---|---|---|
| ID 1 | 6.1% | 7.2% | 11.6% | 12.7% | 1.0% |
| ID 2 | 10.6% | 3.1% | -2.1% | -4.2% | -2.8% |
| ID 3 | -5.2% | -2.2% | -1.3% | 5.3% | -3.2% |

**Table 6. Maximum error about sizing loads subdivided by adimensionalized BL - AW609 HT**

| SZ loads | 0.00 | 0.30 | 0.55 | 0.77 | 1.00 |
|---|---|---|---|---|---|
| ID 1 | 1.8% | -3.1% | -6.3% | -2.8% | 0.7% |
| ID 2 | 5.4% | 10.7% | 12.7% | -10.4% | -2.9% |
| ID 3 | 11.5% | 6.3% | -4.1% | -0.4% | 0.3% |

**Table 7. Maximum error about sizing loads subdivided by adimensionalized STA - AW609 Fin**

| SZ loads | 0.00 | 0.30 | 0.55 | 0.77 | 1.00 |
|---|---|---|---|---|---|
| ID 1 | 2.4% | -0.6% | 6.3% | 0.5% | -4.8% |
| ID 2 | -7.6% | -4.6% | 1.7% | -8.3% | 1.6% |
| ID 3 | 10.2% | 8.7% | 5.5% | 6.0% | 4.8% |

**Table 8. Maximum error about sizing loads subdivided by adimensionalized STA - AW139 Fuselage**

| SZ loads | 0.00 | 0.23 | 0.35 | 0.64 | 1.00 |
|---|---|---|---|---|---|
| ID 1 | 7.3% | 3.9% | 1.0% | 1.2% | 3.9% |
| ID 2 | -2.2% | 2.4% | 2.7% | 1.4% | 0.9% |
| ID 3 | 5.1% | 4.9% | 4.7% | 3.5% | 0.3% |

**Table 9. Maximum error about sizing loads subdivided by adimensionalized BL - NGCTR-TD Wing**

| SZ loads | 0.00 | 0.11 | 0.46 | 0.74 | 1.00 |
|---|---|---|---|---|---|
| ID 1 | 10.3% | 10.6% | 4.2% | 3.6% | 4.6% |
| ID 2 | 3.7% | 4.4% | -5.8% | 3.6% | 0.3% |

**Table 10. Maximum error about sizing loads subdivided by adimensionalized STA - NGCTR-TD Fuselage**

| SZ loads | 0.00 | 0.23 | 0.35 | 0.64 | 1.00 |
|---|---|---|---|---|---|
| ID 1 | 54.3% | 54.5% | 4.5% | 4.6% | 2.0% |
| ID 2 | 40.9% | 29.7% | 44.6% | 21.7% | 1.6% |
| ID 3 | 9.8% | 3.5% | 1.8% | 2.2% | 3.0% |

**Table 11. Maximum error about sizing loads subdivided by adimensionalized STA - NGCTR-TD Fin**

| SZ loads | 0.00 | 0.30 | 0.55 | 0.77 | 1.00 |
|---|---|---|---|---|---|
| ID 1 | -1.3% | -9.5% | -13.1% | 6.1% | 0.03% |
| ID 2 | -1.4% | -0.9% | -17.3% | 7.8% | 0.2% |